The Electrical Breakdown of Thin Dielectric Elastomers

Thermal Effects

Zakaria, Shamsul Bin; Morshuis, Peter H. F.; Yahia, Benslimane Mohamed; Gernaey, Krist; Skov, Anne Ladegaard

Published in:
Proceedings of SPIE

Link to article, DOI:
10.1117/12.2037292

Publication date:
2014

Document Version
Publisher's PDF, also known as Version of record

The Electrical Breakdown of Thin Dielectric Elastomers: Thermal Effects

Zakaria Shamsul[a], Peter H. F. Morshuis[b], Benslimane Mohamed Yahia[c], Krist V. Gernaey[d], Anne Ladegaard Skov[*a]

a: Danish Polymer Center, Department of Chemical and Biochemical Engineering, Technical University of Denmark, Søltofts Plads, Building 229, 2800 Kgs. Lyngby.

b: Faculty of Electrical Engineering, Mathematics and Computer Science, Technology University of Delft, Mekelweg 4, 2628 CD Delft, The Netherland.

c: Danfoss Polypower A/S, Nordborgvej 81 DK-6430 Nordborg.

d: Center for Process Engineering and Technology, Department of Chemical and Biochemical Engineering, Technical University of Denmark, Søltofts Plads, Building 229, 2800 Kgs. Lyngby.

ABSTRACT

Dielectric elastomers are being developed for use in actuators, sensors and generators to be used in various applications, such as artificial eye lids, pressure sensors and human motion energy generators. In order to obtain maximum efficiency, the devices are operated at high electrical fields. This increases the likelihood for electrical breakdown significantly. Hence, for many applications the performance of the dielectric elastomers is limited by this risk of failure, which is triggered by several factors. Amongst others thermal effects may strongly influence the electrical breakdown strength.

In this study, we model the electrothermal breakdown in thin PDMS based dielectric elastomers in order to evaluate the thermal mechanisms behind the electrical failures. The objective is to predict the operation range of PDMS based dielectric elastomers with respect to the temperature at given electric field. We performed numerical analysis with a quasi-steady state approximation to predict thermal runaway of dielectric elastomer films. We also studied experimentally the effect of temperature on dielectric properties of different PDMS dielectric elastomers. Different films with different percentages of silica and permittivity enhancing filler were selected for the measurements. From the modeling based on the fitting of experimental data, it is found that the electrothermal breakdown of the materials is strongly influenced by the increase in both dielectric permittivity and conductivity.

Keywords: DEAP, PDMS, electrothermal breakdown, numerical method

1. INTRODUCTION

The advantages of the dielectric electroactive polymer (DEAP) technology such as flexibility, lightweight and relatively low cost[1] make them outperforming pneumatics and electromagnetics in many ways[2]. Even with the DEAP technology being at a maturing level, it is believed to possess huge potential for inclusion into mainstream products[3].

For electrical insulation systems in high-voltage applications such as power cables, the mechanisms of the electrical breakdown in these solid insulators have been discussed for several decades. Several factors that might lead to electrical breakdown such as intrinsic breakdown, thermal breakdown, electromechanical breakdown and partial discharge breakdown have been studied extensively[4]. Even though power cable and DEAP are operated at high electrical fields, the differences in functionalities, applications and properties make them distinct from each other. Thus, current studies of the mechanisms of electrical breakdown in DEAP are important and in line with the development of DEAP technology and certainly this information can give numerous benefits especially for the manufacturers. For instance, in the early 1960s,

* al@kt.dtu.dk; phone +45 4525 2825

polyethylene was chosen as an insulator for power cables[5]. This hydrophobic material[6] was assumed to be a perfect insulator at that time. However, after a few years in service the cables started to break down[5]. Therefore, the investigations were performed to elucidate the mechanisms behind this failure. The investigations showed that the cable encountered water degradation which now is well-known as 'water treeing'. Consequently, many solutions for avoiding water treeing were introduced such as lead shields, swelling powders and triple extrusion in order to prevent moisture inside the cable and thereby reduce the water treeing problem considerably[4].

In solid dielectrics, electrical breakdown may be thermal which means it is caused by the fact that heat generated within the film cannot be dissipated sufficiently and thereby leads to thermal instability[4]. The heat balance equation is given by[7]

$$C\frac{dT}{dt} = \sigma(E,T)E^2 + \nabla(K(T)\nabla T) \quad (1)$$

where C is volumetric heat capacity, T is temperature, t is time, E is electrical field, ∇ is the Laplace operator, K(T) is the temperature dependent thermal conductivity, and σ(E,T) is field and temperature dependent electrical conductivity.

In thin dielectric films, when the power dissipation increases rapidly with increasing applied voltage, a critical voltage will be reached at a certain point. Whitehead[8] termed this 'the maximum thermal voltage', i.e. the voltage before thermal runway occurs. Analytical and numerical theories to predict thermal runway for thin dielectric films have been developed. For instance, Xiaoguang et al. (2003)[7] studied thermal runway of a thin polypropylene film between two metal electrodes using the finite element method (FEM) where the temperature rise as function of electric fields for 10 μm thick polypropylene film has been computed and the result showed that the temperature increases slowly prior to the critical voltage (875 V/μm) at which thermal runway occurs.

In this study, the thermal effects that may lead to electrical breakdown in thin PDMS film will be modeled. We assume the effect of temperature on electrical breakdown of thin PDMS film is different from polypropylene film as investigated by Xiaoguang et al. (2003)[7]. The main difference is that the PDMS elastomer is chemically crosslinked and thus the Young's modulus will not decrease with temperature as for the thermoplastic. Furthermore, recent studies (Kollosche et al. 2011)[9] have shown that the breakdown strength increases with increasing Young's modulus.

The modeling will be based on the experimental data of dielectric permittivity, elasticity and conductivity with varying temperature of PDMS films. Furthermore, thermogravimetric studies will also be performed to evaluate the thermal stability of the materials with no applied electrical field.

2. METHODOLOGY

2.1 The samples

Five different types of silicone elastomers with different loadings of reinforcing silica particles as well as a permittivity enhancing filler (titanium dioxide) were studied. Four of the elastomers are commercially available elastomers of either the type LSR (liquid silicone rubber) or RTV (room temperature vulcanizing). In the following, details are given on how the test specimens were manufactured:

A. Elastosil® LR 3043/30 was obtained from Wacker Chemie AG, Germany and the solvent OS-20 (an ozone-safe volatile methylsiloxane (VMS) fluid) was obtained from Dow Corning®, USA. Elastosil is supplied as a two parts system. The part A contains PDMS and a platinum catalyst, and part B contains PDMS and a cross-linker. The mixing ratio of Elastosil A, B and OS-20 is 5:5:7 by mass, respectively.

B. POWERSIL® XLR® 630 A/B is an extra-low viscosity LSR and supplied as two parts system. Part A contains PDMS and a platinum catalyst, and part B contains PDMS and a cross-linker. The mixing ratio of parts A and B is 1:1. No solvent is added since the viscosity of the XLR formulations allows for coating without solvent.

C. POWERSIL® RT® 625 A/B is a *room-temperature vulcanizing (RTV)* polymer supplied as a two parts system. Part A contains PDMS and a cross-linker, and Part B contains PDMS and a platinum catalyst. The mixing ratio of parts A and B is 9:1. No solvent is added since the viscosity of the RT formulations allows for coating without solvent.

D. Sample V35 is prepared using PDMS chains cross-linked with a 4-functional hydride cross-linker. All the polymers are purchased from Gelest Inc. and the applied molecular weights are supplied by the company. The catalyst platinum, cyclovinylmethyl-siloxane complex (511) is provided by Hanse Chemie. The material is supplied as 2 systems. Part A contains PDMS and cross-linker and Part B contains PDMS and platinum catalyst. The ratio of polymer and crosslinker (r) was set at 1.2. Four ppm catalyst was added to the premixes. The mixing ratio of parts A and B is 1:1 by mass.

E. The POWERSIL® XLR® 630 A/B with filler is a similar type of material as sample A, except for the addition of a filler. The applied filler is 16% Hombitec® RM130F®, hydrophobic titanium oxide from Sachtleben Chemie, Duisburg, Germany. The average primary particle size is 15 nm. The solvent OS-20 (an ozone-safe volatile methylsiloxane (VMS) fluid) was obtained from Dow Corning®, USA.

All samples were prepared based on the procedures described by Skov et al. (2013)[10] as specified below:

A speedmixer DAC 150FVZ (Hauschild Co., Germany) is used to mix premixes for 5 minutes. Glass plates are coated with the different materials using a thin film 3540 bird applicator (Elcometer, Germany). Then, the sample is cured in the oven for 10 minutes at 80°C. The final networks prepared as thin films are removed from the glass plates and stored between 50 μm thickness ethylene-tetrafluorethylen (ETFE) foils, and kept in a dry place until use.

2.2 Rheological and dielectric characterization and thermogravimetric analysis (TGA)

A TA Instruments ARES G2 Rheometer was used to characterize the rheological properties of the prepared films. The instrument was set to a controlled strain mode at 2% strain, which was ensured to be within the linear viscoelastic regime of the applied elastomers. The sample was inserted between two parallel circular plate geometries of 25 mm with a normal force of approximately 3 N. At a frequency of 1.0 Hz, the temperature was varied from 25°C to 450°C. Dielectric characterization was performed on a TA Instruments ARES G2 Rheometer operating at a frequency of 1.0 Hz, with a normal force of 3 N. The sample was inserted between two parallel circular plate geometries of 25 mm and the temperature was varied from 25°C to 450°C. Additionally, the thermogravimetric analysis (TGA) was performed with a TA Q500 equipped with autosampler. The samples were heated in an inert atmosphere (nitrogen gas) up to 900°C and the heating rate was 5°C/min.

2.3 Resistivity test

Volume resistivity measurements were performed in a three-terminal cell by means of a Keithley 617 electrometer. In order to protect the electrometer from overcurrents, the instrument was connected to the measuring electrode via a series resistor. The poling DC voltage was supplied to the sample via a gold-plated electrode. The electrode was held in place by a spring system to ensure good contact with the sample. A personal computer equipped with a General Purpose Interface Bus (GPIB) was used for displaying and storing the acquired data. In table 1, some specifications of the set-up are given. The current density was obtained by means of equation (2), where $i(t)$ is the current measured by the electrometer and A is the area of the measuring electrode. In order to reach the quasi steady-state regime, the DC field had to be applied for a sufficiently long polarization time.

$$j(t) = \frac{i(t)}{A} \tag{2}$$

The quasi steady-state value of the current density, J, was used for calculating the conductivity σ of the insulation via equation (3), where E is the applied electric field. The volume resistivity is the inverse of the conductivity, σ.

$$\sigma = \frac{J}{E} \tag{3}$$

Table 1. The specifications of the conduction current setup for the resistivity test[11]

Measuring electrode diameter	28 mm
HV electrode diameter	35 mm
Guard electrode diameter	350 mm
Sensitivity	$2 \times 10^{-11} AM^{-2}$
Max temperature	80°C
Max voltage	±30 kV
Series resistor	10 MΩ

3.0 RESULT AND DISCUSSION

3.1 Experimental data

In order to evaluate the effect of temperature on the mechanical properties of PDMS film, the storage modulus and tan delta have been measured at elevated temperature and at a frequency of 1.0 Hz. The storage modulus is a measure of the deformation energy stored by the film during the shear process and tan delta, which is also known as the loss factor, is calculated as the ration between the loss modulus and the storage modulus[12].

Figure 1 shows the storage modulus and tan delta as a function of PDMS film temperature. The storage modulus for PDMS film increases significantly, from 106 kPa at 190°C to 580 kPa at 450°C. This indicates that the PDMS film is hardened with increasing temperature. In addition, at 320°C the maximum tan delta (0.4) is shown which indicates a strong relaxation process and high energy dissipation in the film.

On the contrary, as mentioned in Tripathi (2002)[13], the thermoplastic polypropylene film will show a different behavior towards elevated temperature compared to the thermoset silicone elastomer. Therefore, we assumed the difference in rheological properties between PDMS and polypropylene films at high temperature may affect the behavior of both films with respect to electrothermal breakdown.

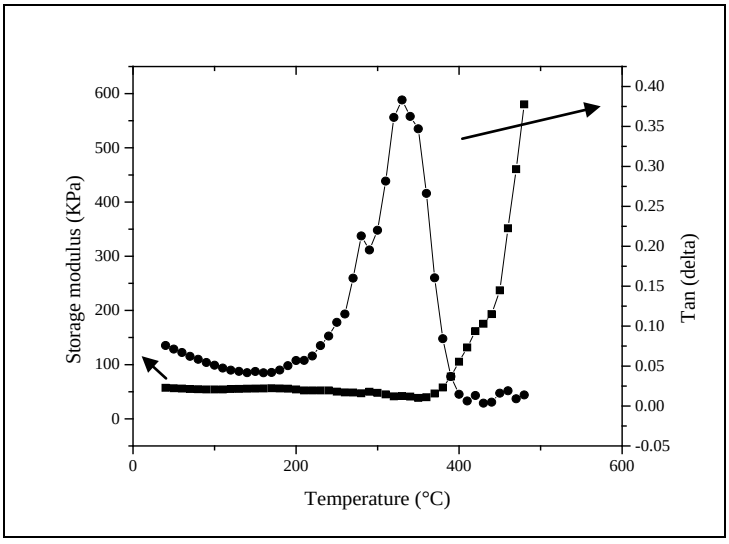

Figure 1. Elastosil LR 3043/30 film with 25 mm diameter and 0.8 mm thickness was used for characterization of the thermal dependence of the rheological properties of PDMS. The storage modulus and the loss tangent are plotted for temperatures between 25°C and 480°C.

Figure 2 shows the storage permittivity (ε') and loss permittivity (ε'') as a function of PDMS film temperature for a temperature range from 25°C to 450°C. The storage and loss permittivity are the real and imaginary part of the permittivity, respectively. The relative dielectric permittivity is given as $\varepsilon_r=\varepsilon'/\varepsilon_o$.

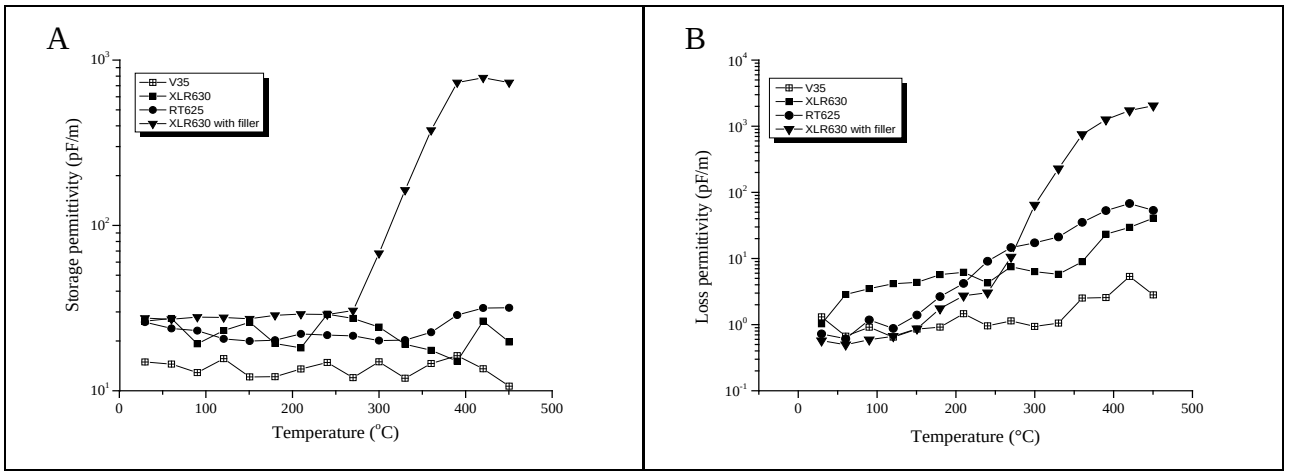

Figure 2. The dielectric properties as function of elevated temperatures for several PDMS films: (A) Storage permittivity (B) Loss permittivity.

Figure 3 shows the electrical conductivity as a function of temperature. The figures clearly indicate an increase in loss permittivity and electrical conductivity of the titanium dioxide loaded PDMS films upon increase of temperature. This can be attributed to the increased polarizability of the titanium dioxide particles.

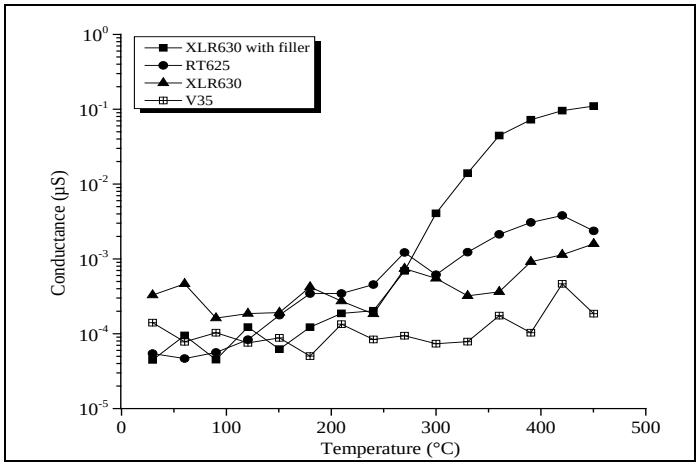

Figure 3. The AC electrical conductivity at 1 Hz as function of temperature for several PDMS films.

The increase of the loss permittivity with increasing temperature is attributed to more dissipation of the electrical energy into heat[14]. At the same time, the increase of electrical conductivity at the more elevated temperature causes more heat production since the joule heating is directly proportional to the electrical conductivity[4]. Therefore, these properties are likely to affect the electrothermal breakdown behavior in PDMS film. Hence, a model that evaluates the effect of temperature and electric field dependence of electrical conductivity on electrothermal breakdown in PDMS film has been applied in this study and will be discussed in the next section.

The purpose of the TGA analysis is to determine the percentages of silica and filler loaded into various PDMS films and also to determine if electrothermal breakdown occurs before film degradation. Figure 4 illustrates different percentages of weight loss at 900°C for all PDMS films. This behavior is believed to depend on the percentage of silica and filler inside the films which need higher temperature to degrade.

As shown in figures 2 and 3, there is a significant increase in the loss permittivity and the electrical conductivity when the temperature of PDMS films is above 150°C.

In figure 4 TGA results of the different films are shown. TGA provides useful information on the materials since the mass loss upon heating can be measured. A constant mass at elevated temperature indicates thermal stability. Furthermore the filler content (inorganic components) can be estimated from the solid content at elevated temperature (>800°C). Figure 4 illustrates that all the investigated PDMS films start to degrade after 300°C and the data in table 2 indicates the temperature where 2% of weight of the films has been decomposed. This temperature is deemed relevant since it gives an estimate of the point in time when thermal degradation sets off. Two of the films, namely RT625 and XLR with filler, possess relatively low 2% degradation temperatures (around 300°C) whereas the other two have to be heated above 400°C before significant degradation takes place. Therefore, if the electrothermal breakdown occurs above these characteristic temperatures, it will be a combined – probably accelerated – process of both thermal decomposition as well as electrothermal runaway. The RT625 formulation is most sensitive to degradation at 300-500°C where the degradation occurs more or less constantly.

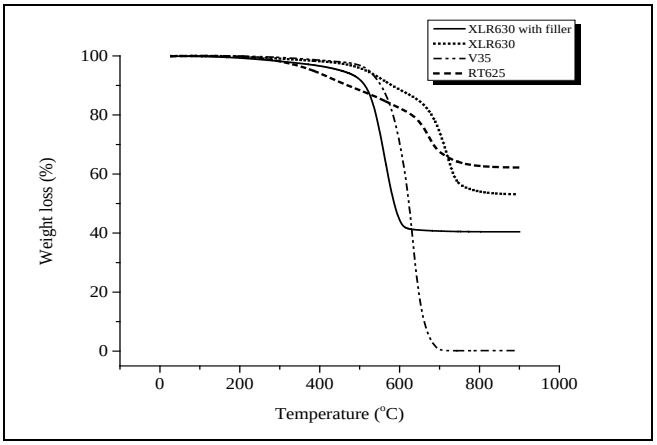

Figure 4. TGA thermograms of PDMS films with different percentages of silica and permittivity enhancing filler.

Table 2. The temperature where 2% of weight of the films has degraded.

PDMS films	Temperature at 2% of weight loss (°C)
XLR630 with filler	313
XLR630	419
V35	451
RT625	305

3.2 Numerical Prediction of Electrothermal Breakdown

For a PDMS film, the volumetric Joule heating from the applied voltage across the film can be calculated as[8]

$$P = \sigma E^2 \tag{4}$$

where σ is the electrical conductivity and E is the electric field. In this model we assume that voltage across the film is increased in small increments, as well as that thermal steady state is reached at each voltage step. The surface temperatures were fixed and the initial temperature and boundary temperatures were set to room temperature.

In order to model the electrothermal breakdown of thin PDMS based dielectric elastomers, the σ should be expressed as function of temperature (T) and electric field (E). Therefore, a linear interpolation of the σ(T) and the σ(E) was calculated to establish an expression of σ(T,E) from the data in figure 5. The interpolation of the electrical dependence is very rough due to the scarcity of experimental data on such systems.

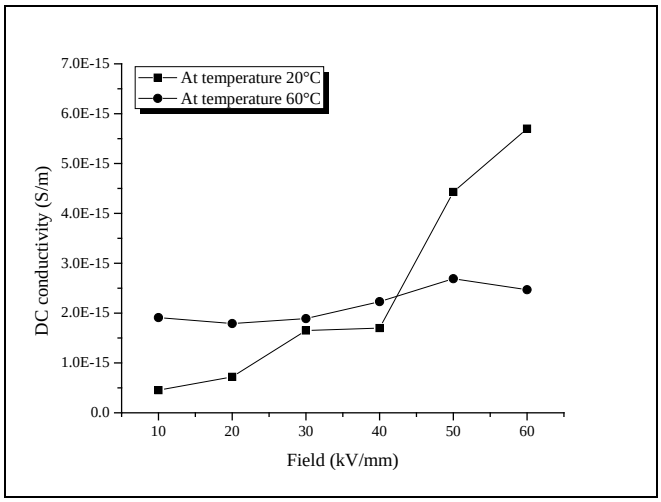

Figure 5. The conductivity as function of the electric fields at two different temperatures for RT625 film. There is a big difference between results at room temperature and at 60°C. These data were used to model the correlation of electrical conductivity with temperature and electric fields.

For computational purposes, we assume that thermal conductivity, *K*, of the PDMS film is 0.15 W/mK[15], that the initial temperature is 300 K and that the expression for electrical conductivity is derived from the data in figure 5 as illustrated below:

The linear equation for DC conductivity versus electric field

$$\text{at } 20°\text{C} : \sigma(\text{E}) = 7.60 \times 10^{-16}\text{E} + 1.95 \times 10^{-16} \tag{5}$$

and

$$\text{at } 60°\text{C} : \sigma(\text{E}) = 1.90 \times 10^{-16}\text{E} + 4.88 \times 10^{-17} \tag{6}$$

The linear graphs were plotted from the slopes (7.60×10^{-16} and 1.90×10^{-16}) and the y-intercepts (1.95×10^{-16} and 4.88×10^{-16}) from the above equations. Then, the linear equations from the graphs were calculated as shown below

$$\sigma(\text{T}) = -2.32 \times 10^{-18}\text{T} + 1.52 \times 10^{-16} \tag{7}$$

and

$$\sigma(\text{T}) = 7.20 \times 10^{-17}\text{T} - 2.74 \times 10^{-15} \tag{8}$$

Lastly the expression of electrical conductivity as function of temperature and electric field is given by

$$\sigma(\mathrm{T},\mathrm{E}) = (-2.32\times10^{-18}\mathrm{T} + 1.52\times10^{-16})\mathrm{E} + 7.20\times10^{-17}\mathrm{T} - 2.74\times10^{-15} \quad (9)$$

As illustrated in figure 6, with the electric field applied along the *x* axis, the thickness of the film was given by ***l***, one boundary of the film is at *x*=0, another boundary at *x*=*l*. The temperature distribution at steady state is then given by[16]

$$dT = \frac{P}{2K}\left(x(l-x)\right) \quad (10)$$

where K is the polymer thermal conductivity and P is the averaged volumetric Joule heating. dT is the incremental change in temperature[16]. Then the average film temperature was calculated in order to be applied in computing a new average electrical conductivity (σ).

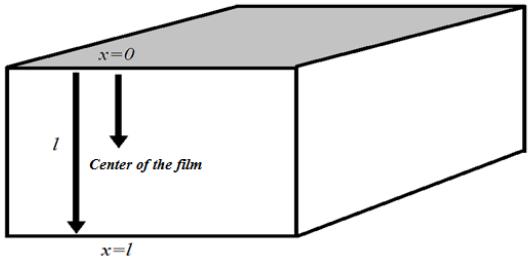

Figure 6: The PDMS film where *l* represents the thickness of the film and *x* represents the position where the electrothermal breakdown field is measured. The maximum temperature will be achieved at the center of the film ($x=\frac{l}{2}$) as predicted by Xiaoguang et al.(2003)[7].

Figure 7 shows the general behavior of temperature versus electric field for PDMS film for which the temperature at the center of the sample just before thermal runway is only a few degrees above the boundary temperature. With only a few volts increase across the sample, thermal runaway occurs very rapidly. The results of this work demonstrate that the thermally induced breakdown fields are significantly higher than the electrical breakdown strengths typically reported for PDMS which are in the range from 19 to 133 V/μm[17].

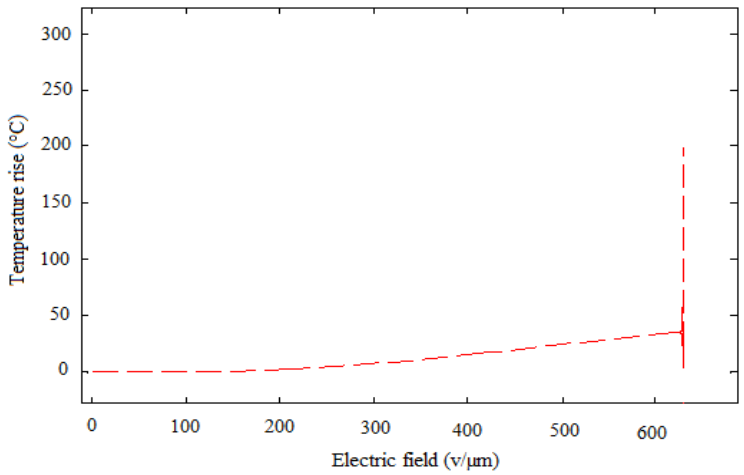

Figure 7. The temperature rise (dT) versus electric field for 50 μm thick PDMS film as computed by the quasi-steady state numerical method. The temperature increases slowly prior to the critical field (629V/μm), at which thermal runaway occurs.

Figure 8 shows the breakdown field as function of electrical conductivity for 50 μm thick PDMS film. The plot illustrates that higher electrical conductivity causes a lower breakdown field, as expected. Practically, this has the implication that electrothermal breakdown is relevant at room temperature as well when the electrical conductivity of the material is high.

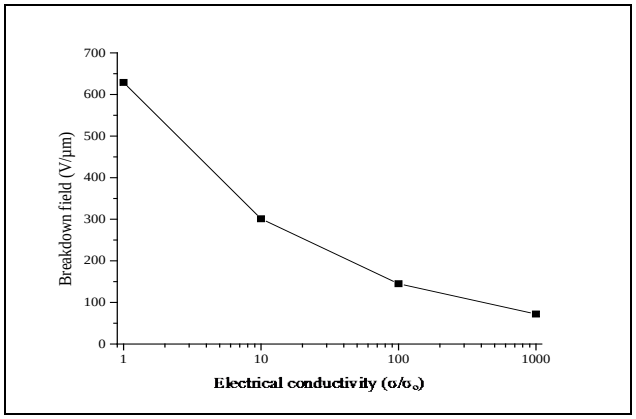

Figure 8. Breakdown fields as function of normalized conductivity at room temperature for the 50 μm thick PDMS film as computed by the quasi-steady state numerical method. The initial electrical conductivity, σ_0, of the PDMS film is 2.45×10^{-16} S/m at room temperature.

Figure 9(A) shows thermal breakdown strengths measured at different distances from the PDMS film surface. Meanwhile, figure 9(B) shows the effect of film thickness on the breakdown field for PDMS film. Both graphs demonstrate similar trends: The breakdown field exhibits a hyperbolic decrease as the position of *x* is closer to the film surface as the result of the heat generated inside the film can be removed rapidly to the surrounding. This characteristic of electrothermal breakdown in thin polymer films agrees well with the predictions reported by Tröls et al. (2013)[18].

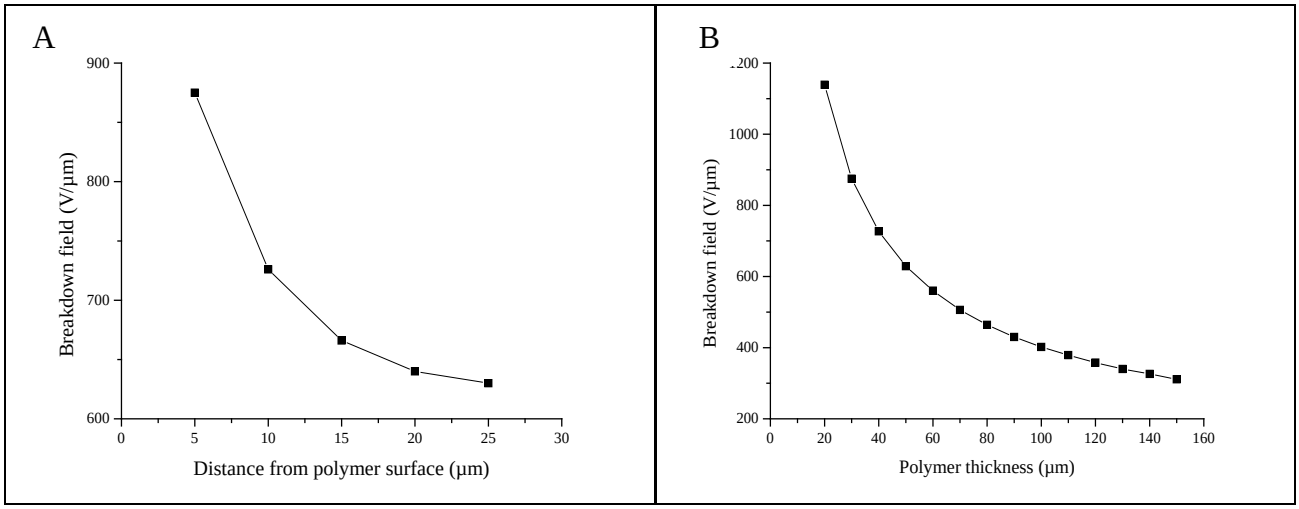

Figure 9. (A) Breakdown strengths at given distances (*x*) from the polymer surface for 50 µm thick PDMS film. (B) The dependence of polymer film thickness on breakdown field computed as described in the text. The value of *x* was fixed as half of the film thickness.

5.0 CONCLUSION

In this study, the effect of temperature on dielectric properties of different systems of PDMS dielectric elastomers has been studied experimentally and a model of electrothermal breakdown in thin PDMS based dielectric elastomers has been applied. From both methods, it can be concluded that electrothermal breakdown of the materials is strongly influenced by the increase in both dielectric permittivity and conductivity. The electrothermal breakdown may not be a major factor to cause electrical breakdown in thin PDMS based dielectric elastomers since the required electrical field required for thermal runaway is about 5 times larger than the reported breakdown fields of silicones.

ACKNOWLEDGEMENT

The authors gratefully acknowledge the financial support from the Ministry of Education of Malaysia and Universiti Malaysia Pahang. Danfoss PolyPower A/S is also acknowledged for financial support to Z. Shamsul.

REFERENCES

[1] R. Shankar, T. K. Ghosh, and R. J. Spontak, "Dielectric elastomers as next-generation polymeric actuators," Soft Matter **3**(9), 1116 (2007).

[2] J. E. Huber, N. A. Fleck, and M. F. Ashby, "The selection of mechanical actuators based on performance indices," Proc. R. Soc. London. Ser. A Math. Phys. Eng. Sci. **453**(1965), 2185–2205 (1997).

[3] Anonymous, [Danfoss PolyPower A/S – White Paper: PolyPower® DEAP actuator elements], Danfoss A/S, Nordborg, Denmark (2012).

[4] J. C. Fothergill and L. A. Dissado, [Electrical degradation and breakdown in polymers], IET (1992).

[5] W. Thue, Electrical power cable engineering, 3rd ed., CRC Press (2012).

[6] M. Ashraf Khan and R. Hackam, "Loss of hydrophobicity of high density polyethylene," in Electr. Insul. Dielectr. Phenomena, 1997. IEEE 1997 Annu. Report., Conf. **2**, pp. 378–381 vol.2 (1997).

[7] Q. Xiaoguang, Z. Zhong, and S. Boggs, "Computation of electro-thermal breakdown of polymer films," in Electr. Insul. Dielectr. Phenomena, 2003. Annu. Report. Conf., pp. 337–340 (2003).

[8] S. Whitehead, [Dielectric breakdown of solids], Clarendon Press Oxford (1951).

[9] M. Kollosche, H. Stoyanov, H. Ragusch, S. Risse, A. Becker, and G. Kofod, “Electrical breakdown in soft elastomers: stiffness dependence in un-pre-stretched elastomers,” in 2010 10th IEEE Int. Conf. Solid Dielectr., pp. 1–4 (2010).
[10] A. L. Skov, S. Vudayagiri, and M. Benslimane, “Novel silicone elastomer formulations for DEAPs,” in SPIE Smart Struct. Mater. Nondestruct. Eval. Heal. Monit., pp. 86871I–86871I–8, International Society for Optics and Photonics (2013).
[11] T. Andritsch, R. Kochetov, Y. T. Gebrekiros, U. Lafont, P. H. F. Morshuis, and J. J. Smit, “Synthesis and dielectric properties of epoxy based nanocomposites,” in Electr. Insul. Dielectr. Phenomena, 2009. CEIDP ’09. IEEE Conf., pp. 523–526 (2009).
[12] T. G. Mezger, [The rheology handbook: for users of rotational and oscillatory rheometers], Vincentz Network GmbH & Co KG (2006).
[13] D. Tripathi, [Practical guide to polypropylene [electronic resource]], iSmithers Rapra Publishing (2002).
[14] A. R. Von Hippel and A. R. Hippel, [Dielectrics and waves], Artech House (1954).
[15] J. Wu, W. Cao, W. Wen, D. C. Chang, and P. Sheng, “Polydimethylsiloxane microfluidic chip with integrated microheater and thermal sensor,” Biomicrofluidics **3**, 12005 (2009).
[16] H. S. Carslaw and J. C. Jaeger, [Conduction of Heat in Solids], 2nd ed., Oxford University Press (1959).
[17] A. P. Gerratt and S. Bergbreiter, “Dielectric breakdown of PDMS thin films,” J. Micromechanics Microengineering **23**(6), 67001 (2013).
[18] A. Tröls, A. Kogler, R. Baumgartner, R. Kaltseis, C. Keplinger, R. Schwödiauer, I. Graz, and S. Bauer, “Stretch dependence of the electrical breakdown strength and dielectric constant of dielectric elastomers,” Smart Mater. Struct. **22**(10), 104012 (2013).